

The Ptk2-Pma1 pathway enhances tolerance to terbinafine in *Trichophyton rubrum*

Masaki Ishii,¹ Tsuyoshi Yamada,^{2,3} Kazuki Ishikawa,¹ Koji Ichinose,¹ Michel Monod,^{4,5} Shinya Ohata¹

AUTHOR AFFILIATIONS See affiliation list on p. 11.

ABSTRACT The increasing prevalence of dermatophyte resistance to terbinafine, a key drug in the treatment of dermatophytosis, represents a significant obstacle to treatment. *Trichophyton rubrum* is the most commonly isolated fungus in dermatophytosis. In *T. rubrum*, we identified TERG_07844, a gene encoding a previously uncharacterized putative protein kinase, as an ortholog of budding yeast *Saccharomyces cerevisiae* polyamine transport kinase 2 (Ptk2), and found that *T. rubrum* Ptk2 (TrPtk2) is involved in terbinafine tolerance. In both *T. rubrum* and *S. cerevisiae*, Ptk2 knockout strains were more sensitive to terbinafine compared with the wild types, suggesting that promotion of terbinafine tolerance is a conserved function of fungal Ptk2. Pma1 is activated through phosphorylation by Ptk2 in *S. cerevisiae*. Overexpression of *T. rubrum* Pma1 (TrPma1) in *T. rubrum* Ptk2 knockout strain (Δ TrPtk2) suppressed terbinafine sensitivity, suggesting that the induction of terbinafine tolerance by TrPtk2 is mediated by TrPma1. Furthermore, omeprazole, an inhibitor of plasma membrane proton pump Pma1, increased the terbinafine sensitivity of clinically isolated terbinafine-resistant strains. These findings suggest that, in dermatophytes, the TrPtk2-TrPma1 pathway plays a key role in promoting intrinsic terbinafine tolerance and may serve as a potential target for combinational antifungal therapy against terbinafine-resistant dermatophytes.

KEYWORDS dermatophytosis, terbinafine resistance, proton pump, Pma1, Ptk2, omeprazole, *Trichophyton rubrum*

Dermatophytes are fungal pathogens that infect the surface tissues of mammals and other animals, causing symptoms such as itching and nail deformities. Dermatophytes can also exacerbate allergies in patients with asthma, significantly reducing their quality of life (1, 2). Antifungal drugs have been developed for fungal infections, and terbinafine, with its ability to inhibit squalene epoxidase in the ergosterol synthesis pathway, has been a highly effective medicine. However, terbinafine-resistant fungi have emerged in recent years (3–5), and the prevalence of resistant strains is a serious concern for the future treatment of dermatophytosis.

Recently, we reported that resistance to terbinafine is caused by mutations in squalene epoxidase, the target of terbinafine (6). The L393F and F397L mutations in squalene epoxidase are the major causes of terbinafine resistance reported worldwide (3, 6–8). However, therapeutic targets and compounds to alleviate this resistance remain to be identified.

Drug repurposing is the practice of using a therapeutic agent that is already approved for the treatment of another disease. In the field of infectious diseases, drug repurposing has become a significant research strategy to discover effective therapeutics against drug-resistant bacteria (9, 10). Previous reports encourage the application of drug repurposing to aid in the research and development of therapies for dermatophytosis.

In the present study, we found that ablation of the gene encoding the putative protein kinase TERG_07844 in *Trichophyton rubrum* resulted in the decrease of tolerance

Editor Andreas H. Groll, University Children's Hospital Münster, Münster, Germany

Address correspondence to Masaki Ishii, m_ishii@musashino-u.ac.jp, or Shinya Ohata, shiohata@musashino-u.ac.jp.

The authors declare no conflict of interest.

See the funding table on p. 12.

Received 6 December 2023

Accepted 12 March 2024

Published 3 April 2024

Copyright © 2024 Ishii et al. This is an open-access article distributed under the terms of the [Creative Commons Attribution 4.0 International license](https://creativecommons.org/licenses/by/4.0/).

to terbinafine. Our findings suggest that the TERG_07844 gene product has a homologous function to the protein kinase Ptk2 of budding yeast and that the proton pump Pma1 functions downstream of the TERG_07844 gene product in terbinafine tolerance. We also found that omeprazole, a proton pump inhibitor approved for clinical use, potentiated the antifungal effect of terbinafine on terbinafine-resistant isolates. These results suggest that the Ptk2-Pma1 pathway enhances resistance to terbinafine in *Trichophyton rubrum* and could be a potential target for antifungal treatment.

RESULTS

TERG_07844 is involved in terbinafine tolerance

Protein kinases are involved in a wide range of physiological activities, including the regulation of intracellular ion concentrations and responses to external stresses such as antifungal drugs (11). Whole-genome analyses of dermatophytes have revealed a large number of genes encoding kinases of unknown function (12). Among these genes, we focused on several genes that are conserved among dermatophytes and are highly expressed in *T. rubrum* (13–15). In efforts to characterize the deletion mutants of these genes, we found that deletion of TERG_07844 leads to terbinafine sensitivity.

A TERG_07844 knockout strain was generated from the terbinafine-susceptible *T. rubrum* strain CBS118892 by replacing the TERG_07844 open reading frame (ORF) with the neomycin resistance gene (*nptII*) cassette (Δ TERG_07844; Fig. 1A). We also generated a revertant strain (eYFP-TERG_07844C) by random integration of the eYFP-TERG_07844 gene, which expresses the TERG_07844 gene product (XP_047604827) tagged with enhanced yellow fluorescent protein (eYFP) at the N-terminus (eYFP-XP_047604827) to obtain an information of the TrPtk2 subcellular localization, in the genome of Δ TERG_07844.

To confirm the loss of the TERG_07844 ORF, PCR was performed using primer pairs designed within the TERG_07844 ORF (primers 1 and 2 in Fig. 1A) and the neomycin resistance gene *nptII* cassette (primers 3 and 4 in Fig. 1A). PCR using the former primer pair amplified the PCR products in the parental strain CBS118892 and eYFP-TERG_07844C, but not in Δ TERG_07844 (Fig. 1B). Conversely, PCR using the latter primer pair did not amplify the PCR products in CBS118892 but did in Δ TERG_07844 and eYFP-TERG_07844C (Fig. 1C). In eYFP-TERG_07844C, two bands were amplified because of two selection markers, *nptII* and *hph* genes (Fig. 1C). Intracellular eYFP signals in eYFP-TERG_07844C were confirmed by confocal microscopy (Fig. 1D).

To analyze the terbinafine susceptibility of *T. rubrum* CBS118892, Δ TERG_07844, and eYFP-TERG_07844C, we cultured these strains on agar plates in the presence and absence of low concentrations of terbinafine (Fig. 1E and G) and measured the diameter of the colonies (Fig. 1F and H). The mycelial growth of Δ TERG_07844 was comparable to that of CBS118892 and eYFP-TERG_07844C on the agar medium without terbinafine (Fig. 1E and F). However, on agar medium containing terbinafine, the mycelial growth of Δ TERG_07844 was significantly reduced (Fig. 1G and H). These results suggest that TERG_07844 is involved in terbinafine tolerance in *T. rubrum*.

XP_047604827 encoded by TERG_07844 in *T. rubrum* is phylogenetically and functionally similar to *S. cerevisiae* Ptk2

To gain insight into TERG_07844, we performed a phylogenetic tree analysis to determine which kinases in *S. cerevisiae* are similar to XP_047604827 encoded by TERG_07844 (Fig. 2A). The phylogenetic tree revealed that XP_047604827 is grouped with the halotolerance kinases Sat4 (accession number [NP_009934](#)) and Hal5 (accession number [NP_012370](#)) from *S. cerevisiae*. Deficiencies in these kinases result in the decrease of high salt tolerance in *S. cerevisiae* (16). The polyamine transport kinase, Ptk2 (accession number [NP_012593](#)), was also found in proximity to XP_047604827. In contrast to Sat4 and Hal5, the absence of Ptk2 has been reported to cause high salt tolerance in *S. cerevisiae* (17, 18). Near XP_047604827, the protein XP_964224, identified as a Ptk2

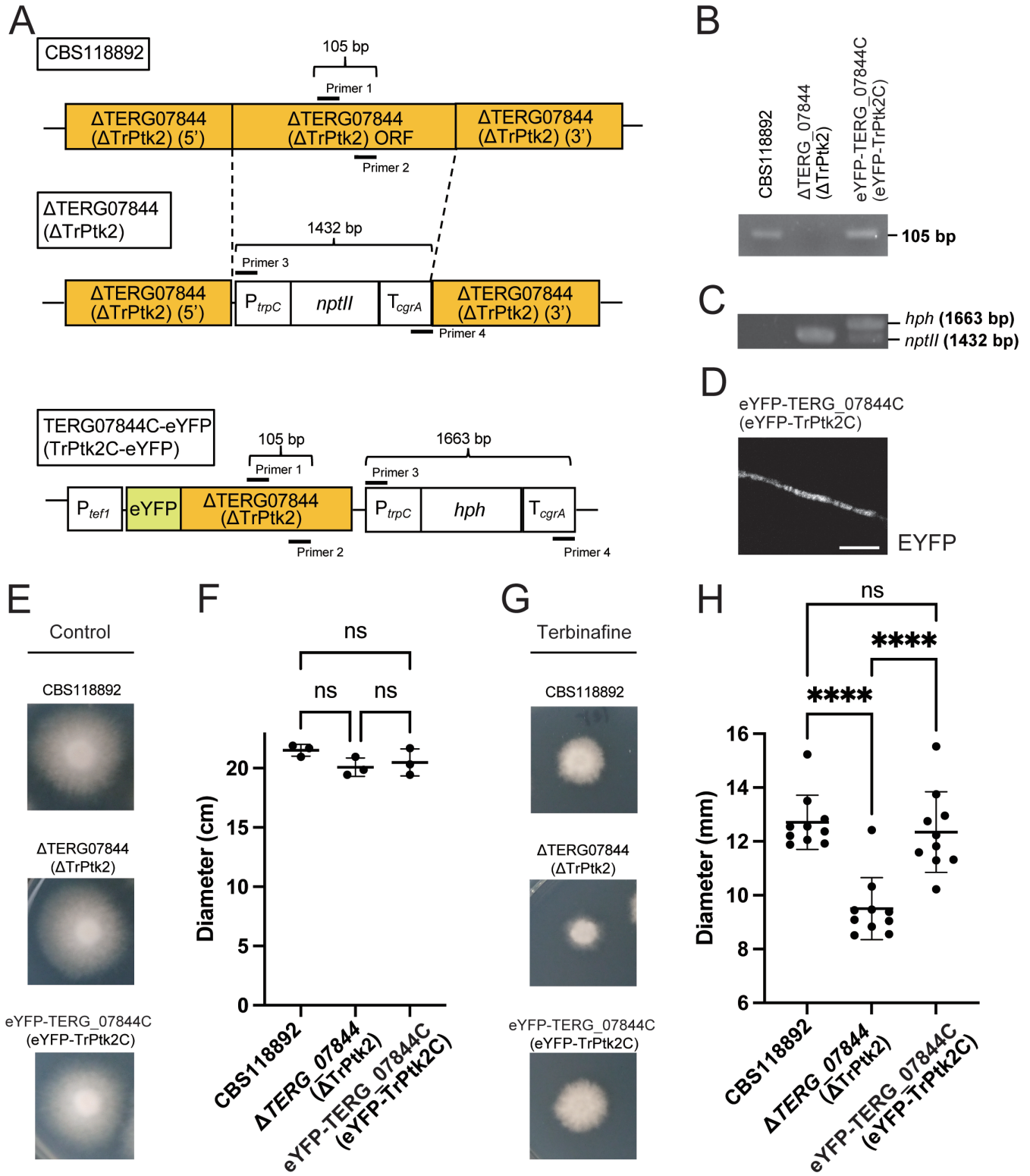


FIG 1 Contribution of the TERG_07844 (TrPtk2) gene to terbinafine sensitivity in *Trichophyton rubrum*. (A) Schematic representation of the TERG_07844 (TrPtk2) wild-type allele (top, CBS118892), deletion construct (middle, ΔTERG_07844), and revertant construct (bottom, eYFP-TERG_07844C). (B) PCR analysis of CBS118892 and ΔTERG_07844 (TrPtk2) and eYFP-TERG_07844C (eYFP-TrPtk2C) using primer pairs 1 and 2. (C) PCR analysis of CBS118892 and ΔTERG_07844 (TrPtk2) and eYFP-TERG_07844C (eYFP-TrPtk2C) using primer pairs 3 and 4. (D) Spores of eYFP-TERG_07844C (eYFP-TrPtk2C) were inoculated on SD for 2 days. The eYFP signals of the sample were observed under confocal microscopy and shown in white. Scale bar is 10 μm. (E–H) Terbinafine susceptibility of CBS118892, (Continued on next page)

FIG 1 (Continued)

Δ TERG_07844, and eYFP-TERG_07844C, in the presence and absence of low concentrations of terbinafine. (E) Spores of CBS118892, Δ TERG_07844 (TrPtk2), and eYFP-TERG_07844C (eYFP-TrPtk2C) were inoculated on RPMI 1640 for 14 days. (F) The diameter of the mycelium on RPMI 1640 after 14 days was measured. The data shown are mean \pm SD. The dots on the graph represent the diameter of individual samples ($n = 3$). (G) Spores of CBS118892, Δ TERG_07844 (TrPtk2), and eYFP-TERG_07844C (eYFP-TrPtk2C) were inoculated on RPMI 1640 with 5 ng/mL of terbinafine for 14 days. (H) The diameter of the mycelium on RPMI 1640 with 5 ng/mL terbinafine after 14 days was measured. The data shown are mean \pm SD. The dots on the graph represent the diameter of individual samples ($n = 10$).

ortholog in the filamentous fungus *Neurospora crassa* (19), was also found (Fig. 2A). To determine whether XP_047604827 is functionally related to either Sat4/Hal5 or Ptk2, we examined the response of *T. rubrum* Δ TERG_07844 in a medium containing high salt concentrations. Compared with the terbinafine-sensitive strain CBS118892, Δ TERG_07844 exhibited enhanced mycelial growth in the presence of 0.5 M NaCl and displayed high salt tolerance, like the Ptk2-deficient *S. cerevisiae* strain Δ ScPtk2 (17, 18). Moreover, the sensitivity of Δ TERG_07844 to compounds to which Δ ScPtk2 is resistant was investigated (18). The results showed that Δ TERG_07844 is resistant to spermine and lithium chloride (Fig. 2B and C). These salt tolerances were significantly reduced in eYFP-TERG_07844C (Fig. 2B and C). These results suggest that XP_047604827 encoded by TERG_07844 has phylogenetic and functional similarities to the Ptk2 protein of budding yeast. Consequently, we refer to *T. rubrum* XP_047604827 encoded by TERG_07844 as TrPtk2 in this study.

To investigate the general impact of fungal Ptk2 on terbinafine resistance, we assessed the sensitivity of the Ptk2-deficient *S. cerevisiae* strain Δ ScPtk2 (Table 1) to terbinafine. As previously reported, Δ ScPtk2 was resistant to spermine (Fig. 2D, left and center panels). Interestingly, Δ ScPtk2 was sensitive to terbinafine (Fig. 2D, right panel), similar to Δ TrPtk2 (Fig. 1H). These observations suggest that the contribution of fungal Ptk2 to terbinafine tolerance is evolutionarily conserved in fungi.

Overexpression of TrPma1 suppresses the terbinafine sensitivity of Δ TrPtk2

In *S. cerevisiae*, the proton pump Pma1 is an essential protein for fungal growth (20). Pma1 is the most established substrate of Ptk2 and is activated by this kinase through phosphorylation in *S. cerevisiae* (21, 22). To investigate if TrPma1 functions downstream of TrPtk2, we overexpressed TrPma1 tagged with eYFP at its C-terminus (TrPma1-eYFP) in Δ TrPtk2 and examined whether TrPma1 could complement the terbinafine sensitivity of Δ TrPtk2. On terbinafine-free agar medium (control), *T. rubrum* CBS118892 (parent), Δ TrPtk2, eYFP-TrPtk2C (revertant), and TrPma1OE-eYFP (Δ TrPtk2 overexpressing TrPma1-eYFP) (Table 1) showed similar growth rates (Fig. 3A). Mycelial growth was inhibited in *T. rubrum* Δ TrPtk2 not only on agar media containing terbinafine but also on agar media containing other squalene epoxidase inhibitors, namely, liranaftate and butenafine. Conversely, the mycelial growth in the presence of squalene epoxidase inhibitors was restored in the revertant strain eYFP-TrPtk2C and TrPma1OE-eYFP (Fig. 3A). These results suggest that TrPma1 acts downstream of TrPtk2 in the promotion of squalene epoxidase inhibitor resistance.

Since Pma1 functions as a proton pump on the plasma membrane in *S. cerevisiae* (23), TrPtk2 could potentially enhance resistance to terbinafine by regulating the subcellular localization of TrPma1. We overexpressed TrPma1-eYFP in CBS118892 and Δ TrPtk2, then cultivated these strains with or without terbinafine, and examined the subcellular localization of TrPma1-eYFP (Fig. 3B). In CBS118892, TrPma1-eYFP localized to the fungal cell surface, as reported for other fungal Pma1 (Fig. 3B). The membrane localization of TrPma1-eYFP was not affected in this strain cultured on terbinafine-containing agar medium, indicating that terbinafine does not disrupt the subcellular localization of TrPma1-eYFP. The localization of TrPma1-eYFP on the fungal cell surface was not disrupted in Δ TrPtk2 in the presence or absence of terbinafine. These results suggest that TrPtk2 is not involved in the regulation of TrPma1 subcellular localization and that TrPtk2

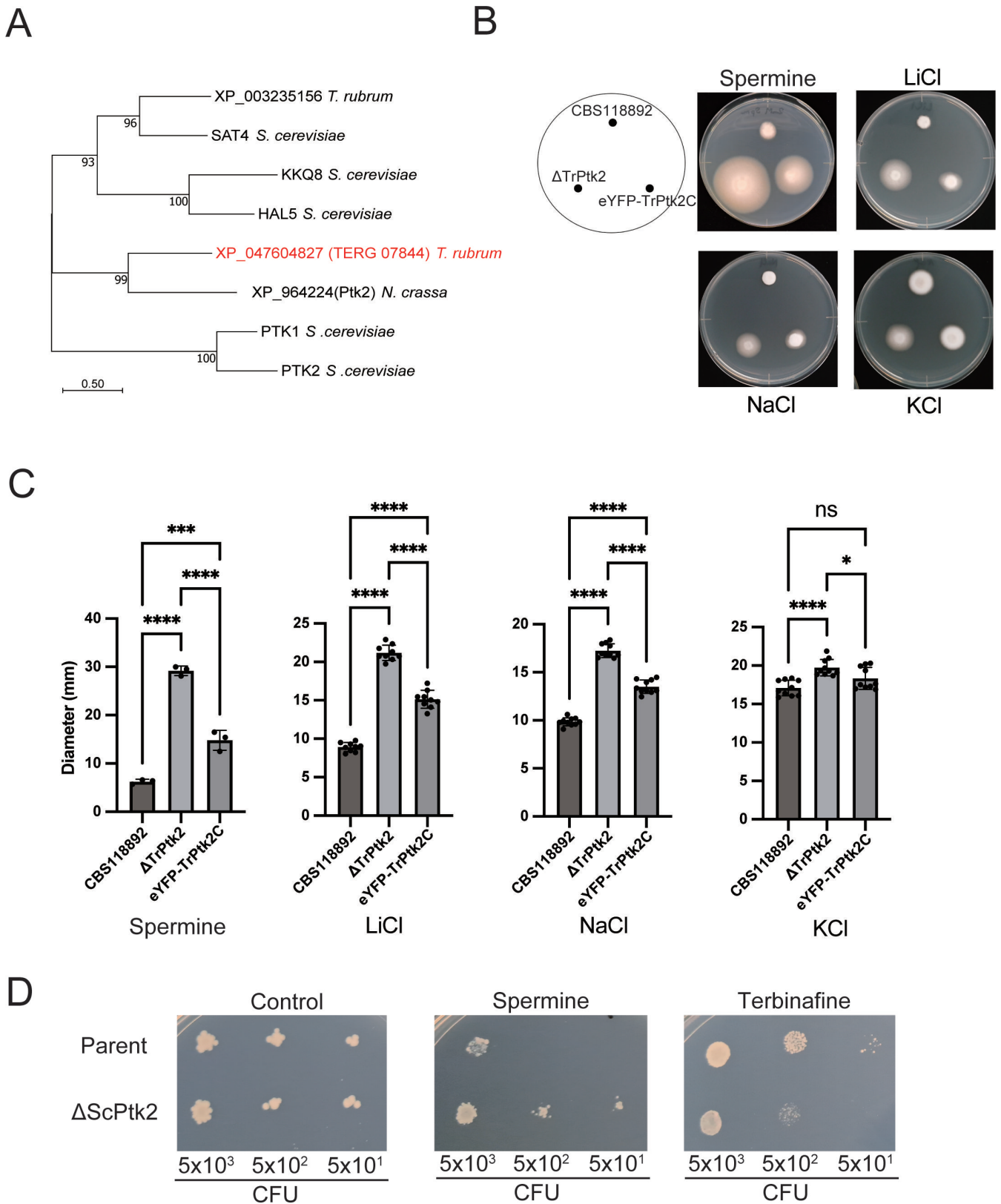


FIG 2 TERG_07844 gene product XP_047604827 of *T. rubrum* is phylogenetically and functionally similar to Ptk2. (A) Phylogenetic tree of fungal proteins related to XP_047604827 (TrPtK2) encoded by TERG_07844 inferred using the maximum likelihood method. The optimal tree is displayed. Evolutionary distances were estimated using the JTT model. (B–C) Effect of spermine and various salts on TERG_07844 (TrPtK2) growth. Spores of CBS118892, ΔTERG_07844 (TrPtK2), and (Continued on next page)

FIG 2 (Continued)

eYFP-TERG_07844C (eYFP-TrPtk2C) were inoculated on SDA with 2 mM spermine, 50 mM LiCl, 0.5 M NaCl, and 0.5 M KCl and incubated for 14 days (B). The diameter of the mycelium was measured (C). The data shown are mean \pm SD. The dots on the graph represent the diameter of individual samples ($n = 3$ for spermine; $n = 10$ for others). (D) Acquired resistance of *S. cerevisiae* to spermine and susceptibility to terbinafine after deletion of the gene encoding Ptk2. Parent and Δ ScPtk2 were grown in synthetic defined medium, and serial dilutions were dropped on synthetic defined agar plates with 2 mM spermine or 50 μ g/mL terbinafine. Growth was measured after 3 days.

promotes terbinafine tolerance by a mechanism other than the regulation of TrPma1 subcellular localization.

Omeprazole enhances the antifungal activity of terbinafine in both terbinafine-susceptible and resistant strains

TrPtk2 inhibitors may be effective compounds for combination therapy for dermatophytosis, as Δ TrPtk2 displayed greater sensitivity to terbinafine compared with the terbinafine-susceptible strain CBS118892 (Fig. 1F and G). However, no fungal Ptk2 inhibitors have been identified to date. We hypothesized that pharmacological inhibition of Pma1 might improve dermatophyte sensitivity to terbinafine, since TrPma1 functions downstream of TrPtk2 (Fig. 3C). We assessed the growth characteristics of CBS118892 on agar medium containing terbinafine and omeprazole, an inhibitor of Pma1 in the yeast (24). Terbinafine alone had a significant inhibitory effect on the mycelial growth of CBS118892 dermatophytes (Fig. 4A and B). Furthermore, the combination of omeprazole and terbinafine resulted in greater inhibition of mycelial growth than either omeprazole or terbinafine treatment alone (Fig. 4A and B). These results suggest that omeprazole increases the terbinafine sensitivity of terbinafine-susceptible dermatophyte strains.

The resistance of *T. rubrum* to terbinafine is mainly due to specific mutations in the squalene epoxidase. The mutations L393F and F397L showed the highest minimum inhibitory concentrations (7). We investigated if omeprazole could enhance terbinafine sensitivity in resistant strains. For this purpose, we used clinical isolates of terbinafine-resistant strains that had specific mutations in the squalene epoxidase gene. These included strain TIMM20092 with the F397L mutation and strains TIMM20093 and TIMM20094, both with the L393F mutation (6). In these terbinafine-resistant strains, both omeprazole and terbinafine exhibited inhibition of mycelial growth individually, except for terbinafine-treated TIMM20094, whose mycelial diameter was comparable with that of the vehicle control (Fig. 4C and D). Interestingly, co-administration of terbinafine and omeprazole resulted in more pronounced inhibitory effects than either medicine alone

TABLE 1 Fungal strains used in this study

Species and strains	Description	Reference
<i>Trichophyton rubrum</i>		
CBS118892	A terbinafine-sensitive clinical isolate from a patient nail sample.	(12)
Δ TERG_07844 (Δ TrPtk2)	The TERG_07844 ORF was replaced with the neomycin resistance gene (<i>nptII</i>) in the strain. This strain was derived from CBS118892.	This study
eYFP-TERG_07844C (eYFP-TrPtk2C)	A complementary (revertant) strain by random integration of the N-terminal eYFP tag-fused TERG_07844 gene into the Δ TERG_07844 (Δ TrPtk2) genome.	This study
TrPma1OE-eYFP	Δ TrPtk2 overexpressing eYFP-tagged TrPma1 by random integration of the C-terminal eYFP tag-fused TrPma1 gene into the Δ TERG_07844 (Δ TrPtk2) genome.	This study
TIMM20092	A terbinafine-resistant clinical isolate has a F397L in the squalene epoxidase.	(6)
TIMM20093	A terbinafine-resistant clinical isolate has a L393F in the squalene epoxidase.	(6)
TIMM20094	A terbinafine-resistant clinical isolate has a L393F in the squalene epoxidase.	(6)
<i>Saccharomyces cerevisiae</i>		
Parent	A strain harboring pYES2-HTH derived from BY4741 (purchased from Horizon Discovery Ltd.).	This study
Δ ScPtk2	A strain harboring pYES2-HTH derived from YJR059W (a Ptk2 deletion strain derived from BY4741) (purchased from Horizon Discovery Ltd.).	This study

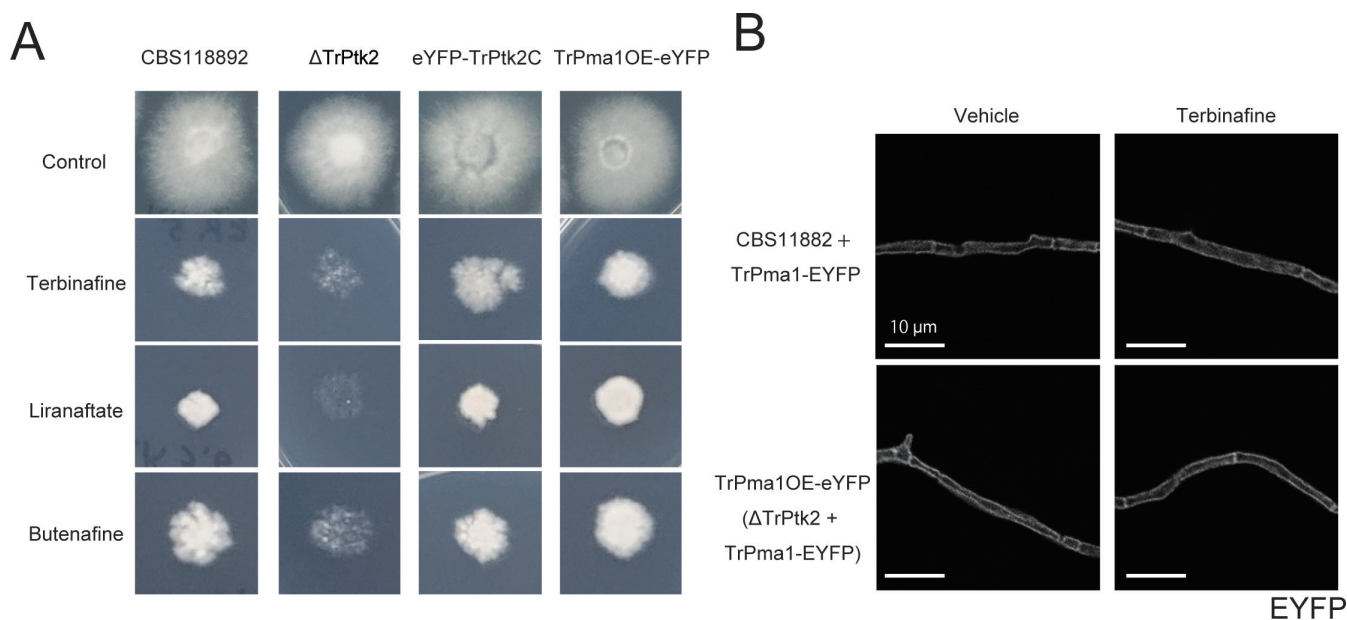


FIG 3 Overexpression of TrPma1 suppresses terbinafine sensitivity of TERG_07844 deletion mutant. (A) Spores of strains were inoculated on RPMI 1640 with 5 ng/mL terbinafine, 6.4 ng/mL liranafate, or 10 ng/mL butenafine and incubated for 14 days. (B) Spores of CBS11882 + TrPma1 eYFP and TrPma1OE-eYFP(Δ TrPtk2 + TrPma1 eYFP) were inoculated on RPMI 1640 and incubated for 2 days or on RPMI 1640 with 0 or 1 μ g/mL terbinafine for 3 h. The eYFP signals of the sample were observed under confocal microscopy and shown in white. Scale bars are 10 μ m.

(Fig. 4C and D). These results suggest that omeprazole enhances terbinafine sensitivity even in terbinafine-resistant dermatophytes.

DISCUSSION

The present study suggests that the fungal Ptk2-Pma1 pathway promotes tolerance to squalene epoxidase inhibitors, including terbinafine (Fig. 5). Although terbinafine has potent antifungal activity on its own, the finding in this study that inhibition of the TrPtk2-TrPma1 pathway enhances the efficacy of terbinafine is clinically important in terms of overcoming terbinafine-resistant strains. Inhibition of the ATPases, including kinases and proton pumps, has recently emerged as a novel therapeutic approach against drug-resistant dermatophytes (25). Our finding that the antifungal efficacy of terbinafine against terbinafine-resistant dermatophytes is enhanced by omeprazole underscores the importance of this strategy. The veterinary antiparasitic milbemycin has been reported to promote the activity of the antifungal drugs itraconazole and voriconazole via inhibition of the dermatophyte efflux pump MDR3 (26). Omeprazole, which was found to enhance the antifungal effect of terbinafine in this study, has an advantage over milbemycin in terms of clinical applicability as it is a drug approved for human use. This study also suggests that compounds that potentiate the activity of antifungals can be found by repurposing non-antifungal drugs.

Based on the studies in *S. cerevisiae* (21, 22), we propose that TrPma1 functions downstream of TrPtk2 in the promotion of tolerance to terbinafine. Consistent with this idea, we observed that the terbinafine susceptibility of *T. rubrum* was increased when TrPma1 was inhibited by omeprazole and that the terbinafine sensitivity of the TrPtk2 mutant was ameliorated upon TrPma1 overexpression. Nevertheless, it remains inconclusive whether and how TrPtk2 functions upstream of TrPma1 in *T. rubrum*, as these observations could have a different basis. In future studies, it will be important to demonstrate the TrPtk2-dependent phosphorylation of TrPma1 in *T. rubrum* and that the activity of TrPma1 depends on TrPtk2. In addition, the molecular mechanism by which the fungal Ptk2-Pma1 pathway contributes to terbinafine tolerance remains unknown. As

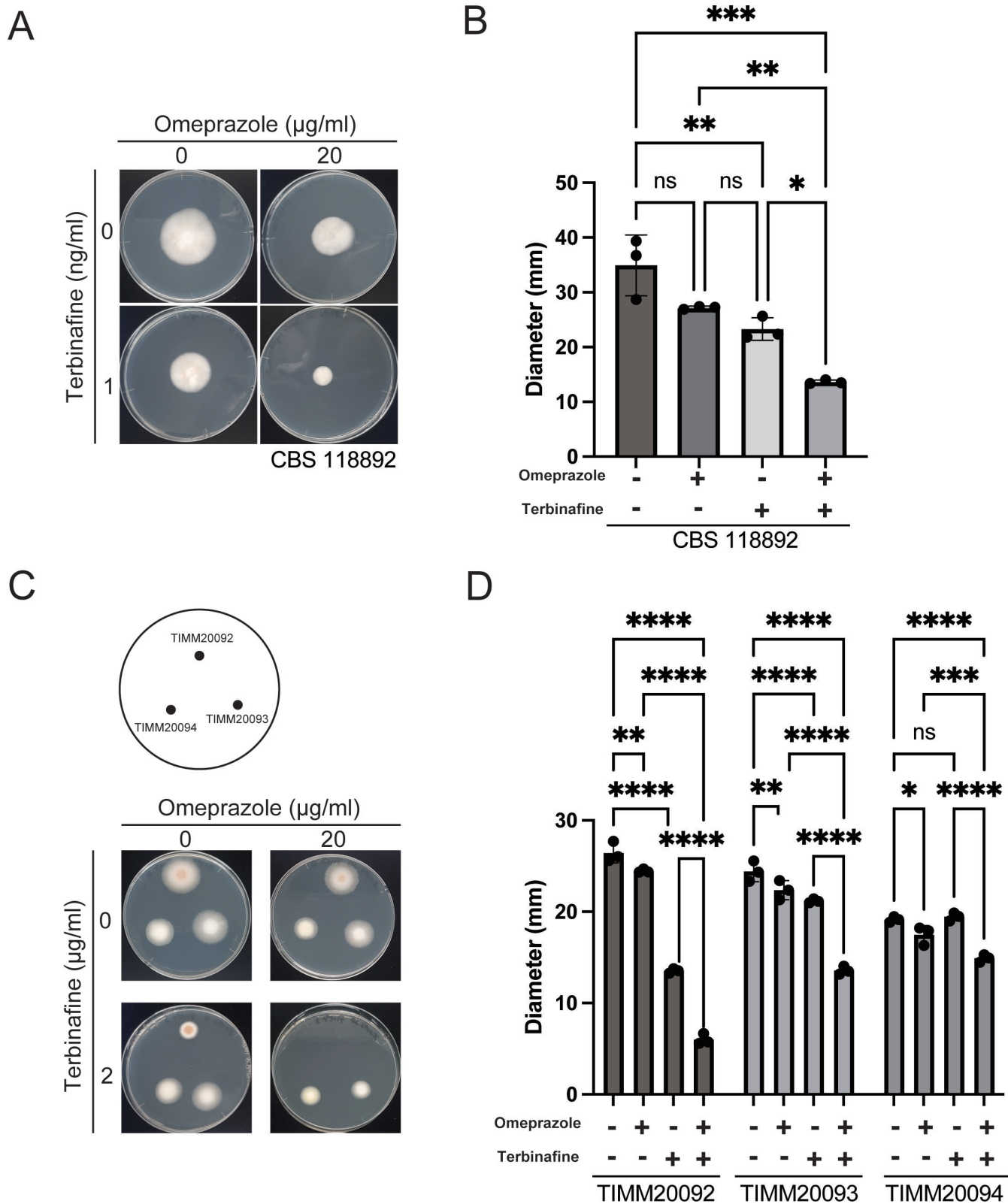


FIG 4 The proton pump inhibitor, omeprazole, enhances the antifungal activity of terbinafine in terbinafine-resistant isolates. (A and B) Combination of omeprazole and terbinafine resulted in greater inhibition of mycelial growth than either omeprazole or terbinafine treatment alone. (A) Spores of CBS118892 were inoculated on SDA with 0 or 20 $\mu\text{g/ml}$ omeprazole and/or 1 ng/mL terbinafine and incubated for 15 days. (B) The diameters of the mycelium on SDA with 0 or 20 $\mu\text{g/ml}$ omeprazole and/or 1 ng/mL terbinafine were measured after 15 days of incubation. The data shown are mean \pm SD. The dots on the graph represent (Continued on next page)

FIG 4 (Continued)

the diameter of individual samples ($n = 3$). (C and D) Decreased terbinafine resistance in terbinafine-resistant isolates in the presence of omeprazole. (C) Spores of TIMM20092, TIMM20093, and TIMM20094 were inoculated on SDA with 0 or 20 $\mu\text{g}/\text{mL}$ omeprazole and/or 2 $\mu\text{g}/\text{mL}$ terbinafine and incubated for 10 days. (D) The diameters of the mycelium on SDA with 0 or 20 $\mu\text{g}/\text{mL}$ omeprazole and/or 2 $\mu\text{g}/\text{mL}$ terbinafine were measured after 10 days of incubation. Since TIMM20092 cultured on SDA agar with 20 $\mu\text{g}/\text{mL}$ omeprazole and 2 $\mu\text{g}/\text{mL}$ terbinafine showed almost no mycelial growth, the diameter was designated as the diameter of the original spot. The data shown are mean \pm SD. The dots on the graph represent the diameter of individual samples ($n = 3$).

there was no change in the subcellular localization of TrPma1-EYFP in the TrPtk2 mutant, TrPtk2 control of TrPma1 was not through regulation of the subcellular localization of TrPma1. In *S. cerevisiae*, Pma1 is phosphorylated by Ptk2 and exports protons from the cell (21, 22). The drug: H^+ antiporter major facilitator superfamily (MFS) in budding yeast requires the proton gradient that crosses the plasma membrane for drug efflux (27). TrPtk2 may phosphorylate TrPma1, thereby facilitating the formation of the proton gradient necessary for the drug efflux pump to export terbinafine. An efflux pump MDR2 has been identified as a transporter for terbinafine excretion in dermatophytes (28). Since TrPtk2 has also been reported to promote polyamine, Na^+ , and Li^+ uptake (29–31), it is possible that the TrPtk2-TrPma1 pathway contributes to the acquisition of terbinafine resistance by other mechanisms. Further functional analysis of the TrPtk2-TrPma1 pathway is necessary to better understand terbinafine resistance in dermatophytes. The increased sensitivity to terbinafine of the ΔScPtk2 strain of *S. cerevisiae* lacking Ptk2 demonstrated in this study will also allow *S. cerevisiae* to be used for further studies as a genetic analysis tool alongside studies in *T. rubrum*.

The terbinafine-resistant dermatophyte isolates used in this study have the L393F and F397L substitution mutations in squalene epoxidase (6). The ability of omeprazole to enhance the antifungal activity of terbinafine against these clinical isolates with the major known resistance mutations is critical for therapeutic applications. Furthermore, we found that all three squalene epoxidase inhibitors used in the present study exhibited enhanced antimicrobial activity against ΔTrPtk2 compared with the terbinafine-susceptible parent strain CBS118892. The potential enhanced antifungal activities of squalene epoxidase inhibitors other than terbinafine are important for the further analysis of the function of TrPtk2 as a new medication target and its clinical translation.

MATERIALS AND METHODS

Fungal and bacterial strains and culture conditions

Agrobacterium tumefaciens EAT105 (32) was cultured at 28°C in *Agrobacterium* induction medium supplemented with 0.2 mM acetosyringone. Fungal strains used in this study are listed in Table 1. *Trichophyton rubrum* CBS118892, a clinical isolated strain from a patient nail sample, was used (12). Terbinafine-resistant *T. rubrum* isolates (TIMM20092, TIMM20093, and TIMM20094) (6) were cultured at 28°C on Sabouraud dextrose agar (SDA; 1% Bacto peptone, 4% glucose, 1.5% agar, and pH unadjusted) or 0.165 M

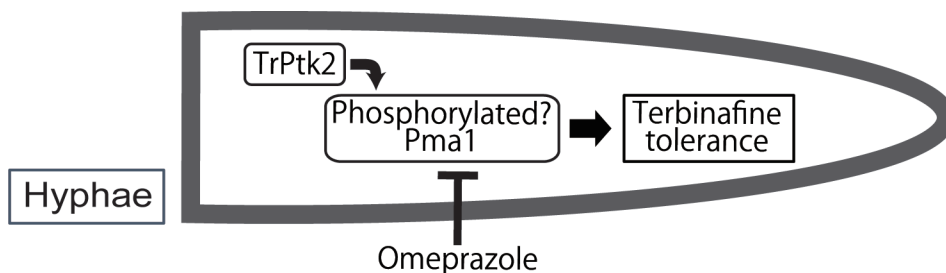


FIG 5 Model of terbinafine tolerance mechanism in *T. rubrum*. Terbinafine tolerance in *Trichophyton rubrum* might be promoted by the phosphorylation of TrPma1 by TrPtk2. The tolerance of *T. rubrum* to terbinafine is decreased by TrPtk2 knockout and omeprazole treatment.

MOPS-buffered RPMI 1640 agar. *S. cerevisiae* BY4741 and YJR059W were purchased from Horizon Discovery Ltd. (California). Parent (BY4741/pYES2-HTH) and Δ ScPtk2 (YJR059W/pYES2-HTH) were cultured at 30°C on yeast extract peptone dextrose (YPD) or synthetic defined medium. Conidia of *T. rubrum* were prepared as described previously (33). pYES2-HTH was purchased from addgene (Massachusetts). For the spot assay, overnight-cultured yeast suspension was diluted with a synthetic defined medium to an optical density of 0.2 ($=1.6 \times 10^6$ CFU/mL). The suspension was serially diluted, and 3 μ L of each suspension was plated onto a synthetic defined agar plate. The samples were incubated at 28°C for 3 days.

Plasmid construction

A TERG_07844 (TrPtk2)-targeting vector, pAg1- Δ TrPtk2, was constructed using the following procedure. First, approximately 1.6-kb fragments of the 5' and 3'-UTR regions of the TERG_07844 ORF were amplified from *T. rubrum* genomic DNA via PCR with specific primer pairs (F: 5'-GAAGGAGTCTTCTCCTGATCTTCAGCCAAGCAGGG-3' and R: 5'-TCAATATCATCTTCTATCGTTCGAGTGGCTTGAGTG-3'; F2: 5'-CGTCATGAATCATCTGCAACTGATCACTGACTGCG-3' and R2: 5'-GTGAATTCGAGCTCGCCCGCAAGATCACAGATCA-3'). The plasmid backbone of pAg and the antibiotic resistance gene cassette were obtained by PCR amplification from the pAg1-3'-UTR of ARB_02021. Finally, these four fragments were fused together using the In-Fusion system (Takara Bio, Inc., Japan).

To construct a vector for TrPtk2 complementation (pCS2-hph-eYFP-TrPtk2), the following steps were performed. First, the antibiotic resistance gene cassette (*hph*) was inserted between the NotI and KpnI sites of pCS2+ N-terminal eYFP, which was generated by inserting the eYFP gene into the BamHI site of pCS2+ (kind gift from S. Kurisu at Tokushima University) (34, 35). Subsequently, the *tef1* promoter (Ptef1) was amplified from the *T. indotineae* genome by PCR with a specific primer pair (F: 5'-GCGGTCGACCCACTAAGACTCCTTCAAGCTCC-3' and R: 5'-GCGAAGCTTGGTGACGGTGATTTTGTGTGG-3') and inserted between the Sall and HindIII sites of the pCS2+ N-terminal eYFP-derived vector. Finally, the TrPtk2 gene was amplified from *T. rubrum* cDNA via PCR using a specific primer pair (F: 5'-GCTGTACAAGGGATCCATGGCCGTTTCGTCTACAT-3' and R: 5'-GTTCTAGAGGCTCGATTAGTTGTAGCCATCGCCCA-3'), and the fragment was inserted between the BamHI and XhoI sites of the above vector.

To construct a vector for TrPma1-eYFP overexpression (pCS2-hph-TrPma1-eYFP), the following steps were performed. First, the antibiotic resistance gene cassette (*hph*) was inserted between the NotI and KpnI sites of pCS2+ C-terminal eYFP (kind gift from S. Kurisu at Tokushima University) (34, 35). Subsequently, the *tef1* promoter (Ptef1) was amplified from the *T. indotineae* genome by PCR with a specific primer pair (F: 5'-GCGGTCGACCCACTAAGACTCCTTCAAGCTCC-3' and R: 5'-GCGAAGCTTGGTGACGGTGATTTTGTGTGG-3') and inserted between the Sall and HindIII sites of the pCS2+ C-terminal eYFP-derived vector. Finally, the *Trpma1* gene was amplified from *T. rubrum* cDNA by PCR using a specific primer pair (F: 5'-TCTTTTTGCAGGATCGCCACCATGGCCGACCACGCAGCC-3' and R: 5'-CCTCTAGAGGCTCGAGGTGCGCTTCTCTGTCTG-3'), and the fragment was inserted between the BamHI and XhoI sites of the above vector.

Transformation of *T. rubrum*

The *A. tumefaciens*-mediated transformation (ATMT) technique was used to alter *T. rubrum*, as previously described (13–15). The concentrations of G418 and hygromycin B for selection were 200 and 600 μ g/mL, respectively. PCR was used to assess the intended transformants and pure genomic DNA. A Quick-DNA Fungal/Bacterial Miniprep Kit (Zymo Research, California) was used to extract the total DNA. The T-01 system (TAITEC, Japan) with 5-mm stainless steel beads was used to perform a study on the collision of beads with fungal cells. For confirmation, PCR was conducted using two primer pairs (primer 1: 5'-GCTTCTCCATCCCTGCTGT-3', primer 2: 5'ATTCTGTGCAAGGGGACAG-3', primer 3:

5'-AGAAGATGATATTGAAGGAGCACTTTTGGGCTT-3', and primer 4: 5'-AGATGATTCATGACGTATATTCACCG-3')

Fluorescent microscopy observation

CBS118892 + TrPma1 eYFP, Δ TERG_07844 + TrPma1 eYFP, or eYFP-TrPtk2C strains were seeded with $1-5 \times 10^6$ spores on sterile cover glasses and placed in a 12-well plate. They were then incubated with 500 μ L of SD liquid medium at 28°C overnight. On the second day, the SD medium was replaced with fresh medium, and the spores were further incubated at 28°C overnight. On the third day, the supernatant was removed, and the cells were cultured in RPMI 1640 with or without terbinafine for 3 h. The sample was fixed with 4% paraformaldehyde (PFA, Nacalai Tesque, Japan) at room temperature for 15 minutes. The samples were washed three times with PBS and mounted on glass slides using Aqua-Poly/Mount (Polysciences, UK). The stained cells were observed using a confocal microscope system (AX, Nikon, Japan).

Phylogenetic tree analysis

The evolutionary history was inferred using the maximum likelihood method and the Whelan and Goldman + Freq. model. The tree with the highest log likelihood (-13,606.41) was used. The percentage of trees in which the associated taxa clustered together was shown below the branches. The initial trees for the heuristic search were obtained automatically by applying the Neighbor-Join and BioNJ algorithms to a matrix of pairwise distances that were estimated using the JTT model and then selecting the topology with the superior log likelihood value. A discrete Gamma distribution was used to model the evolutionary rate differences among the sites [5 categories (+G, parameter = 5.3335)]. The tree was drawn to scale, with branch lengths measured in the number of substitutions per site. This analysis involved eight amino acid sequences. There was a total of 1,163 positions in the final data set. The evolutionary analyses were conducted in MEGA11 software.

Statistical analysis

The means of the two groups were compared using Student's *t*-test. For three or more groups with a single variable, one-way analysis of variance (ANOVA) with Tukey's post hoc test was conducted. For means of three or more groups with two variables, two-way ANOVA with Tukey's post hoc test was performed. Prism 9 software (GraphPad Software, Boston) was utilized for these statistical analyses. Statistical significance was defined at a *P* value of <0.05. n.s., not significant. *, *P* value <0.05. **, *P* value <0.01. ***, *P* value <0.001. ****, *P* value <0.0001.

ACKNOWLEDGMENTS

The authors thank Dr. S. Kurisu at Tokushima University for providing the pCS2+ N-terminal and C-terminal eYFP plasmids and K. Maru, H. Shimokuri, S. Yahagi, H. Uga, and N. Hori for their technical help.

This work was supported by the Japan Society for the Promotion of Science and Takeda Science Foundation.

AUTHOR AFFILIATIONS

¹Research Institute of Pharmaceutical Sciences, Faculty of Pharmacy, Musashino University, Tokyo, Japan

²Teikyo University Institute of Medical Mycology, Teikyo University, Tokyo, Japan

³Asia International Institute of Infectious Disease Control, Teikyo University, Tokyo, Japan

⁴Department of Dermatology, Centre Hospitalier Universitaire Vaudois, Lausanne, Switzerland

⁵Faculty of Biology and Medicine, University of Lausanne, Lausanne, Switzerland

AUTHOR ORCID*s*Masaki Ishii  <http://orcid.org/0000-0003-0687-3147>Tsuyoshi Yamada  <http://orcid.org/0000-0002-1394-5455>Shinya Ohata  <http://orcid.org/0000-0003-4333-4433>

FUNDING

Funder	Grant(s)	Author(s)
MEXT Japan Society for the Promotion of Science (JSPS)	21K15438, 23K06533	Masaki Ishii
Takeda Science Foundation (TSF)		Shinya Ohata

AUTHOR CONTRIBUTIONS

Masaki Ishii, Conceptualization, Data curation, Funding acquisition, Investigation, Writing – original draft, Writing – review and editing, Methodology | Tsuyoshi Yamada, Data curation, Resources, Writing – review and editing | Kazuki Ishikawa, Investigation, Writing – review and editing, Data curation, Methodology | Koji Ichinose, Writing – review and editing, Methodology | Michel Monod, Data curation, Resources, Writing – review and editing | Shinya Ohata, Conceptualization, Data curation, Funding acquisition, Writing – original draft, Writing – review and editing

DATA AVAILABILITY

For comparison of the gene expression of TERG_07844 and other kinase coding genes in *T. rubrum*, we used transcriptome data from the NCBI database (accession numbers: [GSE134406](https://www.ncbi.nlm.nih.gov/geo/query/acc.cgi?acc=GSE134406), [GSE102872](https://www.ncbi.nlm.nih.gov/geo/query/acc.cgi?acc=GSE102872), and [GSE110073](https://www.ncbi.nlm.nih.gov/geo/query/acc.cgi?acc=GSE110073)).

REFERENCES

- Ward GW, Karlsson G, Rose G, Platts-Mills TA. 1989. *Trichophyton* asthma: sensitisation of bronchi and upper airways to dermatophyte antigen. *Lancet* 1:859–862. [https://doi.org/10.1016/s0140-6736\(89\)92863-8](https://doi.org/10.1016/s0140-6736(89)92863-8)
- Ward GW, Woodfolk JA, Hayden ML, Jackson S, Platts-Mills TAE. 1999. Treatment of late-onset asthma with fluconazole. *J Allergy Clin Immunol* 104:541–546. [https://doi.org/10.1016/s0091-6749\(99\)70321-0](https://doi.org/10.1016/s0091-6749(99)70321-0)
- Suzuki S, Mano Y, Furuya N, Fujitani K. 2018. Discovery of terbinafine low susceptibility *Trichophyton rubrum* strain in Japan. *Biocontrol Sci* 23:151–154. <https://doi.org/10.4265/bio.23.151>
- Osborne CS, Leitner I, Favre B, Ryder NS. 2005. Amino acid substitution in *Trichophyton rubrum* squalene epoxidase associated with resistance to terbinafine. *Antimicrob Agents Chemother* 49:2840–2844. <https://doi.org/10.1128/AAC.49.7.2840-2844.2005>
- Mukherjee PK, Leidich SD, Isham N, Leitner I, Ryder NS, Ghannoum MA. 2003. Clinical *Trichophyton rubrum* strain exhibiting primary resistance to terbinafine. *Antimicrob Agents Chemother* 47:82–86. <https://doi.org/10.1128/AAC.47.1.82-86.2003>
- Yamada T, Maeda M, Alshahni MM, Tanaka R, Yaguchi T, Bontems O, Salamin K, Fratti M, Monod M. 2017. Terbinafine resistance of *Trichophyton* clinical isolates caused by specific point mutations in the squalene epoxidase gene. *Antimicrob Agents Chemother* 61:e00115-17. <https://doi.org/10.1128/AAC.00115-17>
- Blanchard G, Amarov B, Fratti M, Salamin K, Bontems O, Chang Y-T, Sabou AM, Künzle N, Monod M, Guenova E. 2023. Reliable and rapid identification of terbinafine resistance in dermatophytic nail and skin infections. *Acad Dermatol Venereol* 37:2080–2089. <https://doi.org/10.1111/jdv.19253>
- Moreno-Sabater A, Normand AC, Bidaud AL, Cremer G, Foulet F, Brun S, Bonnal C, Ait-Ammar N, Jabet A, Ayachi A, Piarroux R, Botterel F, Houzé S, Desoubreux G, Hennequin C, Dannaoui E. 2022. Terbinafine resistance in dermatophytes: a French multicenter prospective study. *J Fungi (Basel)* 8:220. <https://doi.org/10.3390/jof8030220>
- Miyashita A, Mitsutomi S, Mizushima T, Sekimizu K. 2022. Repurposing the PDMA-approved drugs in Japan using an insect model of staphylococcal infection. *FEMS Microbes* 3:xtac014. <https://doi.org/10.1093/femsmc/xtac014>
- Liu Y, Tong Z, Shi J, Li R, Upton M, Wang Z. 2021. Drug repurposing for next-generation combination therapies against multidrug-resistant bacteria. *Theranostics* 11:4910–4928. <https://doi.org/10.7150/thno.56205>
- Caplan T, Lorente-Macías Á, Stogios PJ, Evdokimova E, Hyde S, Wellington MA, Liston S, Iyer KR, Puumala E, Shekhar-Guturja T, Robbins N, Savchenko A, Krysan DJ, Whitesell L, Zuercher WJ, Cowen LE. 2020. Overcoming fungal echinocandin resistance through inhibition of the non-essential stress kinase Yck2. *Cell Chem Biol* 27:269–282. <https://doi.org/10.1016/j.chembiol.2019.12.008>
- Martinez DA, Oliver BG, Gräser Y, Goldberg JM, Li W, Martinez-Rossi NM, Monod M, Shelest E, Barton RC, Birch E, et al. 2012. Comparative genome analysis of *Trichophyton rubrum* and related dermatophytes reveals candidate genes involved in infection. *mBio* 3:e00259-12. <https://doi.org/10.1128/mBio.00259-12>
- Petrucelli MF, Peronni K, Sanches PR, Komoto TT, Matsuda JB, Silva Junior W da, Belebony RO, Martinez-Rossi NM, Marins M, Fachin AL. 2018. Dual RNA-Seq analysis of *Trichophyton rubrum* and HaCat keratinocyte co-culture highlights important genes for fungal-host interaction. *Genes (Basel)* 9:362. <https://doi.org/10.3390/genes9070362>
- Mendes NS, Bitencourt TA, Sanches PR, Silva-Rocha R, Martinez-Rossi NM, Rossi A. 2018. Transcriptome-wide survey of gene expression changes and alternative splicing in *Trichophyton rubrum* in response to undecanoic acid. *Sci Rep* 8:2520. <https://doi.org/10.1038/s41598-018-20738-x>
- Martins MP, Silva LG, Rossi A, Sanches PR, Souza LDR, Martinez-Rossi NM. 2019. Global analysis of cell wall genes revealed putative virulence factors in the dermatophyte *Trichophyton rubrum*. *Front Microbiol* 10:2168. <https://doi.org/10.3389/fmicb.2019.02168>

16. Mulet JM, Leube MP, Kron SJ, Rios G, Fink GR, Serrano R. 1999. A novel mechanism of ion homeostasis and salt tolerance in yeast: the Hal4 and Hal5 protein kinases modulate the Trk1-Trk2 potassium transporter. *Mol Cell Biol* 19:3328–3337. <https://doi.org/10.1128/MCB.19.5.3328>
17. Erez O, Kahana C. 2002. Deletions of SKY1 or PTK2 in the *Saccharomyces cerevisiae* Δ trk2 mutant cells exert dual effect on ion homeostasis. *Biochem Biophys Res Commun* 295:1142–1149. [https://doi.org/10.1016/S0006-291X\(02\)00823-9](https://doi.org/10.1016/S0006-291X(02)00823-9)
18. Goossens A, de La Fuente N, Forment J, Serrano R, Portillo F. 2000. Regulation of yeast H⁺-ATPase by protein kinases belonging to a family dedicated to activation of plasma membrane transporters. *Mol Cell Biol* 20:7654–7661. <https://doi.org/10.1128/MCB.20.20.7654-7661.2000>
19. Lew RR, Kapishon V. 2009. Ptk2 contributes to osmoadaptation in the filamentous fungus *Neurospora crassa*. *Fungal Genet Biol* 46:949–955. <https://doi.org/10.1016/j.fgb.2009.09.005>
20. Serrano R, Kielland-Brandt MC, Fink GR. 1986. Yeast plasma membrane ATPase is essential for growth and has homology with (Na⁺ + K⁺), K⁺ and Ca²⁺-ATPases. *Nature* 319:689–693. <https://doi.org/10.1038/319689a0>
21. Eraso P, Mazón MJ, Portillo F. 2006. Yeast protein kinase Ptk2 localizes at the plasma membrane and phosphorylates *in vitro* the C-terminal peptide of the H⁺-ATPase. *Biochim Biophys Acta* 1758:164–170. <https://doi.org/10.1016/j.bbame.2006.01.010>
22. Lecchi S, Nelson CJ, Allen KE, Swaney DL, Thompson KL, Coon JJ, Sussman MR, Slayman CW. 2007. Tandem phosphorylation of Ser-911 and Thr-912 at the C terminus of yeast plasma membrane H⁺-ATPase leads to glucose-dependent activation. *J Biol Chem* 282:35471–35481. <https://doi.org/10.1074/jbc.M706094200>
23. Morsomme P, Slayman CW, Goffeau A. 2000. Mutagenic study of the structure, function and biogenesis of the yeast plasma membrane H⁺-ATPase. *Biochim Biophys Acta* 1469:133–157. [https://doi.org/10.1016/S0304-4157\(00\)00015-0](https://doi.org/10.1016/S0304-4157(00)00015-0)
24. Monk BC, Mason AB, Abramochkin G, Haber JE, Seto-Young D, Perlin DS. 1995. The yeast plasma membrane proton pumping ATPase is a viable antifungal target. I. Effects of the cysteine-modifying reagent omeprazole. *Biochim Biophys Acta* 1239:81–90. [https://doi.org/10.1016/0005-2736\(95\)00133-n](https://doi.org/10.1016/0005-2736(95)00133-n)
25. Ishii M, Matsumoto Y, Yamada T, Uga H, Katada T, Ohata S. 2023. TrCl4 promotes actin polymerization at the hyphal tip and mycelial growth in *Trichophyton rubrum*. *Microbiol Spectr* 11:e0292323. <https://doi.org/10.1128/spectrum.02923-23>
26. Monod M, Feuermann M, Salamin K, Fratti M, Makino M, Alshahni MM, Makimura K, Yamada T. 2019. *Trichophyton rubrum* azole resistance mediated by a new ABC transporter, TruMDR3. *Antimicrob Agents Chemother* 63:e00863-19. <https://doi.org/10.1128/AAC.00863-19>
27. Costa C, Dias PJ, Sá-Correia I, Teixeira MC. 2014. MFS multidrug transporters in pathogenic fungi: do they have real clinical impact. *Front Physiol* 5:197. <https://doi.org/10.3389/fphys.2014.00197>
28. Fachin AL, Ferreira-Nozawa MS, Maccheroni W, Martinez-Rossi NM. 2006. Role of the ABC transporter TruMDR2 in terbinafine, 4-nitroquinoline N-oxide and ethidium bromide susceptibility in *Trichophyton rubrum*. *J Med Microbiol* 55:1093–1099. <https://doi.org/10.1099/jmm.0.46522-0>
29. Kaouass M, Audette M, Ramotar D, Verma S, De Montigny D, Gamache I, Torossian K, Poulin R. 1997. The STK2 gene, which encodes a putative Ser/Thr protein kinase, is required for high-affinity spermidine transport in *Saccharomyces cerevisiae*. *Mol Cell Biol* 17:2994–3004. <https://doi.org/10.1128/MCB.17.6.2994>
30. Nozaki T, Nishimura K, Michael AJ, Maruyama T, Kakinuma Y, Igarashi K. 1996. A second gene encoding a putative serine/threonine protein kinase which enhances spermine uptake in *Saccharomyces cerevisiae*. *Biochem Biophys Res Commun* 228:452–458. <https://doi.org/10.1006/bbrc.1996.1681>
31. Uemura T, Kashiwagi K, Igarashi K. 2007. Polyamine uptake by DUR3 and SAM3 in *Saccharomyces cerevisiae*. *J Biol Chem* 282:7733–7741. <https://doi.org/10.1074/jbc.M611105200>
32. Yamada T, Makimura K, Satoh K, Umeda Y, Ishihara Y, Abe S. 2009. Agrobacterium tumefaciens-mediated transformation of the dermatophyte, trichophyton mentagrophytes: an efficient tool for gene transfer. *Med Mycol* 47:485–494. <https://doi.org/10.1080/13693780802322240>
33. Uchida K, Tanaka T, Yamaguchi H. 2003. Achievement of complete mycological cure by topical antifungal agent NND-502 in guinea pig model of tinea pedis. *Microbiol Immunol* 47:143–146. <https://doi.org/10.1111/j.1348-0421.2003.tb02797.x>
34. Ohata S, Aoki R, Kinoshita S, Yamaguchi M, Tsuruoka-Kinoshita S, Tanaka H, Wada H, Watabe S, Tsuboi T, Masai I, Okamoto H. 2011. Dual roles of notch in regulation of apically restricted mitosis and apicobasal polarity of neuroepithelial cells. *Neuron* 69:215–230. <https://doi.org/10.1016/j.neuron.2010.12.026>
35. Ohata S, Kinoshita S, Aoki R, Tanaka H, Wada H, Tsuruoka-Kinoshita S, Tsuboi T, Watabe S, Okamoto H. 2009. Neuroepithelial cells require fucosylated glycans to guide the migration of vagus motor neuron progenitors in the developing zebrafish hindbrain. *Development* 136:1653–1663. <https://doi.org/10.1242/dev.033290>